

Nonequilibrium roughening transition by two-species particles

S. Park and B. Kahng

Department of Physics and Center for Advanced Materials and Devices, Kon-Kuk University, Seoul 143-701, Korea

We introduce an interface growth model exhibiting a nonequilibrium roughening transition (NRT) from a smooth phase to a rough phase. In the model, particles consist of two species, and deposit or evaporate on one dimensional substrate according to a given dynamic rule. The dynamic rule is assigned for the two cases, the symmetric and the asymmetric case with respect to particle species. For the asymmetric case, some features of NRT are related to directed percolation, while for the symmetric case, NRT leads to a new universality class. We also consider the case where dynamics is restricted to occur in monolayer. This case belongs to the directed Ising universality class.

PACS numbers:05.70Fh,05.70Jk,05.70Ln

Phase transitions in nonequilibrium systems are distinct in their physical properties from ones in equilibrium systems, in general [1]. For example, roughening transition (RT) from a smooth phase to a rough phase in one dimension does not occur in thermal equilibrium systems [2]. In nonequilibrium systems, however, there are a few examples of exhibiting RT even in one dimension, such as the polynuclear growth models [3], the deposition-evaporation model with no evaporation on terrace [4], and the fungal growth model [5]. The common feature of the models is that some aspects of the RT are related to directed percolation (DP) in 1+1 dimensions [6]. On the other hand, DP behavior occurs in many other nonequilibrium systems exhibiting phase transition from active to inactive state [7]. Typical examples would be the monomer-dimer model for the catalytic oxidation of CO [8], the contact process [9], the surface depinning models [10], and the branch-annihilation random walks with odd numbers of offspring [11]. Recently a lot of efforts have been made to search for other systems exhibiting non-DP behavior. As a result, a few examples have been found such as the probabilistic cellular automata model [12], certain kinetic Ising model [13], the interacting monomer-dimer model [14], modified Domany-Kinzel model [15], and the branch-annihilation random walks with even numbers of offspring (BAWe) [11]. All these models except for the BAWe have two equivalent absorbing states indicating the importance of symmetry of the absorbing state to the universality class. Analogous to equilibrium spin models, the non-DP class with two equivalent absorbing states is referred to as the directed Ising (DI) universality class [16].

Recently the stochastic models [3-5] exhibiting nonequilibrium RT (NRT) were introduced, all of which do not possess any absorbing state. When absorbing state is not present, NRT was understood in terms of the spontaneous symmetry breaking of non-conserved order parameter in Refs.[4-5]. In this Letter, we consider the classification of the universality class of NRT with no absorbing state. Analogous to phase transition with absorbing state, we think that the symmetry lying in dynamic rule can replace the role of symmetry of

the absorbing state, and characterizes the universality class. In order to confirm this idea, we study a simple deposition-evaporation model exhibiting NRT, in which particles consist of two species, and its dynamic rule is symmetric with respect to particle species. We also consider an asymmetric version by breaking the symmetry in the dynamic rule. By numerical simulations, it is found that the symmetric and the asymmetric case behave completely distinctively, confirming that NRT is characterized by the symmetry of dynamic rule. Furthermore, some features of NRT such as the density of vacant sites in smooth phase and the growth velocity in rough phase are related to DP for the asymmetric case, while for the symmetric case, they are not related to DI, leading to a new universality class.

The stochastic model we introduce is defined as follows. We consider an interface dynamics with deposition and evaporation processes of particles on one dimensional substrate with the periodic boundary condition. Particles consist of two species, black and gray colored. The dynamics starts from vacuum state, where no particle is in the system. First, a site is selected at random. Next, either deposition or evaporation of a particle is attempted at the selected site with probability q ($q/2$ for black and $q/2$ for gray particle) and $1 - q$, respectively, and the attempt is realized under the two conditions below. First, a restricted solid-on-solid (RSOS) condition is imposed such that height difference between nearest neighboring columns does not exceed one. Second, we consider a ferromagnetic interaction between two nearest neighboring particles in the same layer. The interaction is attractive (repulsive) when they are the same (different) colored. Then a particle with a certain color cannot deposit (evaporate) when both of neighboring particles in the left and the right sides have different (the same) color from its own one as shown in Fig.1. Particle can deposit or evaporate when the colors of two neighboring particles on each sides are alternative, or one (or both) of the neighboring sites is (are) vacant. Symmetric dynamic rule with respect to particle-color generates symmetry in surface configurations; every surface configuration has its corresponding configuration with replacing one species

by the other species as shown in Fig.1.

In an asymmetric version, one-species particles, say black colored, can distinguish the same species from the other species, however, gray particles cannot see colors and regard black particles as the same species. Then a gray particle can deposit (cannot evaporate) even at the site where both of two neighboring particles in each sides are black. Then the symmetry in the dynamic rule breaks up, and the gray flourish more than the black. As an extreme case of the asymmetric version, when particles are of single species, the model is reduced to the one by Alon *et al* [4], where particles cannot evaporate at any site in terrace, and only can do at the edge of the terrace. The model defined so far is called the growth model to distinguish itself from the model below, called the monolayer model, confined in monolayer.

When the dynamics is restricted on monolayer, so that particle cannot deposit on top of particle, the model exhibits a phase transition from active state to absorbing state. In this case, vacant site means active site, and site occupied by black or gray particle means inactive site. There are two types of inactive sites according to colors. Absorbing state is formed when the entire system is filled with single species of particles. Then there exist two absorbing states which are equivalent as long as the dynamic rule is symmetric with respect to particle species. Thus, it is expected that the phase transition of the monolayer model is in the DI universality class. Our monolayer model is similar to the generalized contact process proposed by Hinrichsen [15], however, our growth model is much simpler because it includes one control-parameter rather than two.

For the growth model, when q is small, a smooth phase is maintained. In this phase, particles form small-sized islands which disappear after their short lifetime. Thus the growth velocity is zero in the thermodynamic limit. As q increases, deposition increases and typical islands grow, until, above a critical value q_c , islands merge and full new layers are completed, giving the interface a finite growth velocity. Accordingly, surface exhibits NRT from a smooth phase to a rough phase across q_c . We measure the density of vacant sites $\rho_g(q, t)$ averaged over all runs, where the subscript g means the growth model. $\rho_g(q, t)$ is saturated at a finite value for $q < q_c$ and decreases to zero exponentially for $q > q_c$ in the long time limit as shown in Fig.2(a). At criticality, $\rho_g(q_c, t)$ scales algebraically as

$$\rho_g(q_c, t) \sim t^{-\beta/\nu_{\parallel}}. \quad (1)$$

We performed Monte Carlo simulations for various system sizes $L = 10 \sim 1000$, and examined the power-law behavior by scanning the probability q . For the asymmetric case, q_c is estimated as $q_c \approx 0.3796$, and $\beta/\nu_{\parallel} \approx 0.160(1)$ is measured, which is in good agreement with the DP values, $\beta/\nu_{\parallel}(DP) \approx 0.1595$ [7]. For the symmet-

ric case, q_c is estimated as $q_c \approx 0.4480$. $\beta/\nu_{\parallel} \approx 0.589(3)$ is measured in the long time limit, which is much deviated from the DI value, $\beta/\nu_{\parallel}(DI) \approx 0.27 \sim 0.29$ [12-17]. We think that this discrepancy may come from the suppression-effect by particle on upper layer; For example, particle A in Fig.1 can evaporate in version of the monolayer model because one of neighboring particles has different color, however, it cannot evaporate in the growth model because of another particle on top of it. On the other hand, for the asymmetric case, the particle A cannot evaporate even in the monolayer model, because two particles on each side are regarded as the same species. Therefore, the suppression-effect appears strongly (weakly) for the symmetric (asymmetric) case. When number of particles on upper layers is relatively small for $q < q_c$, or in the short time regime for $q = q_c$, the suppression-effect is relatively weak. Thus, $\rho_g(q_c, t)$ decays according to the DI behavior in the short time regime as can be seen in Fig.2(a). However, in the long time limit at q_c , lots of particles are on upper layer, and $\rho_g(q_c, t)$ decays as $\sim t^{-0.568}$, faster than the DI behavior.

We consider the probability $S(t)$ that the system contains at least one vacant site on bottom layer, and other sites are occupied by any species of particles. As can be seen in Fig.2(b), there seems to be a characteristic time τ_g such that for $t < \tau_g$, $S(t) = 1$, and for $t > \tau_g$, $S(t)$ decays in the same way as does ρ_g . Thus the density of vacant sites $\rho_g^{(s)}(q_c, t)$ averaged over samples with at least one vacant site is finite beyond τ_g as shown in Fig.2(c). The characteristic time τ_g depends on system size as $\tau_g \sim L^{1.64(2)}$ for the symmetric case. For $q \ll q_c$, τ_g is relatively long, indicating that the dynamics on bottom layer continues. At q_c , τ_g is relatively short, indicating that the dynamics proceeds on upper layer. Thus the suppression is effective. The steady-state density $\rho_g(q, \infty)$ for $\epsilon \equiv (q_c - q) > 0$ may be written as $\rho_g(q, \infty) \sim \epsilon^{\beta}$. According to the scaling theory, there would be a typical time, $\tau(q) \sim (q_c - q)^{-\nu_{\parallel}}$ such that for $t < \tau$, $\rho_g(q, t)$ behaves algebraically as Eq.(1) with the same power, 0.589, and for $t > \tau$, $\rho_g(q, t)$ depends on finite system size. However, this scaling assumption is not valid, because the value of β/ν_{\parallel} for $q < q_c$ appears smaller than 0.589, rather it is close to the DI value as can be seen in Fig.2(a). Accordingly, as can be seen in plot of $\rho_g(q, \infty)$ versus ϵ in Fig.2(d), the data do not fit well to a straight line for small ϵ , but are likely to approach a line asymptotically with slope $\beta \approx 0.88$, the DI value, for large ϵ , being far from q_c . Therefore, the dynamics near q_c of the smooth phase does not follow the DI behavior.

In the rough phase, surface grows with finite velocity, which behaves as $v \sim (q - q_c)^y$. The velocity would be characterized by the inverse of the characteristic time τ_g to complete one layer, $v \sim a/\tau_g$, where a is lattice constant. If τ_g is regarded as being the characteristic time

τ_m for the monolayer model to reach the absorbing state, $\tau_m \sim (q - q_c)^{-\bar{\nu}_{\parallel}}$, where the symbol of bar means the monolayer model, then the velocity exponent y would be equal to $\bar{\nu}_{\parallel}$. This assumption is confirmed numerically by that $y \approx 1.67(8)$ is measured, being close to the DP value, $\nu_{\parallel}(DP) \approx 1.73$ for the asymmetric case. However, for the symmetric case, $y \approx 1.25(3)$ is measured as shown in Fig.3(a), which is obviously deviated from the DI value, $\nu_{\parallel}(DI) \approx 3.17$ [14]. This discrepancy implies that for the symmetric case, the dynamics in the rough phase such as the growth velocity is not related to the dynamics in submonolayer regime of surface growth.

Next, we also consider the surface fluctuation width, $W^2(L, t) = \frac{1}{L} \sum_i h_i^2(t) - \left(\frac{1}{L} \sum_i h_i(t) \right)^2$, where $h_i(t)$ denotes height at site i at time t . The interface width behaves as

$$W^2(L, t) \sim \begin{cases} t^{2\zeta/z}, & \text{for } t \ll L^{1/z}, \\ (-\epsilon)^{\chi} L^{2\zeta}, & \text{for } t \gg L^{1/z}, \end{cases} \quad (2)$$

where ζ and z are called the roughness and the dynamic exponent, respectively. χ is the exponent describing the vanishing of the roughness as the transition is approached. The exponent χ is measured as $\chi \approx 0.34(1)$ ($\approx 0.89(4)$) for the symmetric (asymmetric) case as shown in Fig.3(b). The asymmetric value is close to the value 0.92 obtained from the single-species model [4]. The roughness exponent ζ is measured to be $\zeta \approx 0.50(1)$, which is very close to the value of the Edwards-Wilkinson (EW) universality class [18] and the Kardar-Parisi-Zhang (KPZ) universality class [19] in one dimension. The value of $\zeta \approx 0.5$ is also obtained from the height-height correlation function, $C^2(r) = \langle (h(r) - h(0))^2 \rangle \sim r^{2\zeta}$ in the long time limit as shown in Fig.3(c). The growth exponent ζ/z exhibits a broad range of numerical values from $1/4$ to $1/3$ as the probability q increases as shown in Fig.3(d). Since the velocity for $q > q_c$ is nonzero, the EW universality class for surface growth has to be excluded. Nevertheless, since the velocity is extremely small near q_c , the EW behavior appears numerically for finite system, but in the thermodynamic limit, surface growth for $q > q_c$ is expected to belong to the KPZ class. At q_c , the roughness of surface exhibits the marginal behavior, $W^2 \sim \log t$ for $t \ll L^{1/z}$ and $W^2 \sim \log L$ for $t \gg L^{1/z}$.

Next, we perform numerical simulations for the monolayer model. We start with two distinct initial configurations. First, the initial configuration includes one active site, so that all sites are occupied by a single species particles except one empty site. Then number of active sites increases with increasing time. We measure the survival probability $P(t)$ (the probability that the system is still active at time t), the density of active sites $\rho_m(t)$ averaged over all runs, and the mean-square-distance of spreading of the active region $R^2(t)$ averaged over surviving runs. At criticality, $\bar{q}_c \approx 0.7438$, the values of these quantities scale algebraically in the long time

limit as $P(t) \sim t^{-\bar{\delta}}$, $\rho_m(t) \sim t^{\bar{\eta}}$, and $R^2(t) \sim t^{\bar{z}}$. We measured the exponents as $\bar{\delta} \approx 0.287(1)$, $\bar{\eta} \approx 0.000$, and $\bar{z} \approx 1.141(3)$, all of which are in good agreement with those in the DI universality class [17]. Next, we start with another initial configuration where all sites are empty. This initial configuration is considered for the purpose of comparing with the growth model. In this case, number of active sites decreases with increasing time. Thus, at criticality $\bar{q}_c \approx 0.7490$, the density of active sites behaves as $\rho'_m(t) \sim t^{-\bar{\eta}'}$ and the survival probability does as $P'(t) \sim t^{-\bar{\delta}'}$ with the exponents $\bar{\eta}' \approx 0.290(2)$ and $\bar{\delta}' \approx 0.000$, respectively. Even though the two different initial configurations yield the different values of the exponents, their sum $\bar{\delta} + \bar{\eta}$ seems to be the same as $\bar{\delta}' + \bar{\eta}'$, describing the growth of the number of kinks over surviving samples in the interacting monomer-dimer model [14]. The exponent $\bar{\eta}'$ has different value from β/ν_{\parallel} for the growth model. This result confirms that the growth model with two-species particles generates a new universality class different from the DI universality class. Detailed numerical results for the growth model and the monolayer model will be published elsewhere [20].

In summary, we have introduced an interface growth model with deposition and evaporation of two species particles, exhibiting a nonequilibrium roughening transition (NRT) from a smooth phase to a rough phase as deposition-attempt probability q varies. The dynamic rule of the deposition and evaporation process is assigned symmetrically and asymmetrically with respect to particle species, respectively. For the two cases, NRTs behave distinctively from each other, suggesting that the universality class of NRT is characterized by the symmetry lying in dynamic rule. For the asymmetric case, some features of NRT can be described in terms of directed percolation, while for the symmetric case, the behavior of NRT leads to a new universality class.

BK wish to thank H. Park for helpful discussions. This work was supported in part by the KOSEF through the SRC program of SNU-CTP, and in part by the Ministry of Education, Korea (97-2409).

- [1] For a review, see, V. Privman, *Nonequilibrium phase transitions in lattice models* (Cambridge University, Cambridge, 1996).
- [2] J. D. Weeks, in *Ordering in Strongly Fluctuating Condensed Matter Systems*, edited by T. Riste (Plenum, New York, 1980).
- [3] J. Kertész and D.E. Wolf, Phys. Rev. Lett. **62**, 2571 (1989).
- [4] U. Alon, M.R. Evans, H. Hinrichsen and D. Mukamel, Phys. Rev. Lett. **76**, 2746 (1996); Phys. Rev. E **57**, 4997

(1998).

[5] J. M. López and H. J. Jensen, (cond-mat/9803171).

[6] G. Deutscher, R. Zallen and J. Adler, *Percolation Structures and Processes* Ann. Isr. Phys. Soc. 5 (Adam Hilger, Bristol, 1983).

[7] J. Marro and R. Dickman, in Ref.[1].

[8] R.M. Ziff, E. Gulari and Y. Barshad, Phys. Rev. Lett. **56**, 2553 (1985).

[9] T.E. Harris, Ann. Prob. **2**, 969 (1974); T.M. Liggett, *Interacting Particle Systems* (Springer-Verlag, New York,1985)

[10] A.-L. Barabási and H. E. Stanley, *Fractal Concepts in Surface Growth* (Cambridge University Press, Cambridge, England, 1995); D. Kim, H. Park and B. Kahng, *Dynamics of Fluctuating Interfaces and Related Phenomena* (World Scientific, Singapore, 1997).

[11] H. Takayasu and A. Yu Tretyakov, Phys. Rev. Lett. **68**, 3060 (1992).

[12] P. Grassberger, F. Krause and T. von der Twer, J. Phys. A **17**, L105 (1984).

[13] N. Menyhárd, J. Phys. A **27**, 6139 (1994).

[14] M.H. Kim and H. Park, Phys. Rev. Lett. **73**, 2579 (1994); H. Park and H. Park, Physica A **221**, 97 (1995).

[15] H. Hinrichsen, Phys. Rev. E **55**, 219 (1997).

[16] W. Hwang, S. Kwon, H. Park and H. Park, Phys. Rev. E **57**, 6438 (1998).

[17] N.Inui and A. Yu. Tretyakov, Phys. Rev. Lett. **80**, 5148 (1998).

[18] S.F. Edwards and D.R. Wilkinson, Proc. R. Soc. Lond. A **381**, 17 (1982).

[19] M. Kardar, G. Parisi and Y.C. Zhang, Phys. Rev. Lett. **56**, 889 (1986).

[20] S. Park and B. Kahng, (unpublished).

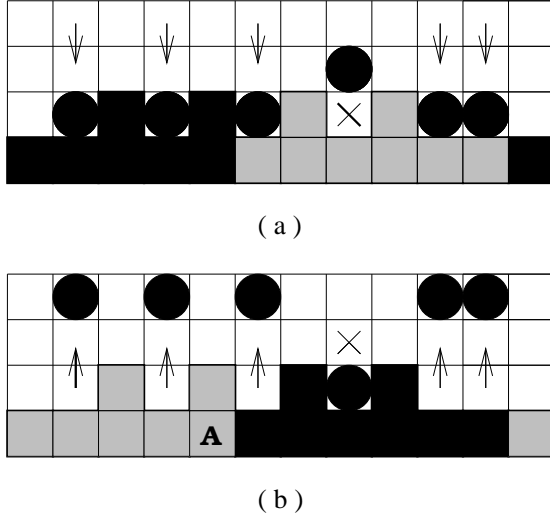


FIG. 1. The dynamic rule for deposition (a) and for evaporation (b) for the symmetric case of the growth model.

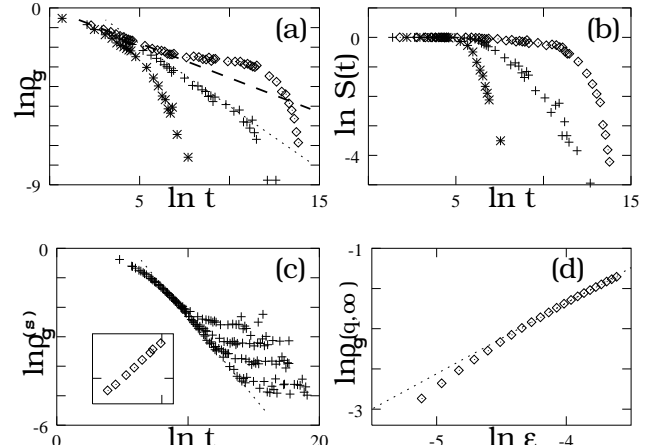


FIG. 2. (a) Double logarithmic plot (DLP) of $\rho_g(q, t)$ versus time t for probabilities $q = 0.4410$ (top), $0.4480 (= q_c)$ and 0.4600 (bottom). The data are obtained for $L = 100$, averaged over more than 500 configurations. The dashed and the dotted lines have slope 0.276 and 0.589, respectively, drawn for the eye. (b) DLP of $S(t)$ versus time t for the same cases as (a). (c) DLP of $\rho_g^{(s)}(q_c, t)$ versus t for different system sizes $L = 50$ (top), 100, 200 and 500. The dotted line has slope 0.589, drawn for the eye. Inset: DLP of τ_g versus L at q_c . (d) DLP of $\rho_g(q, \infty)$ versus ϵ . The dashed line has slope 0.88, drawn for the eye. All plots (a-d) are for the symmetric case of the growth model.

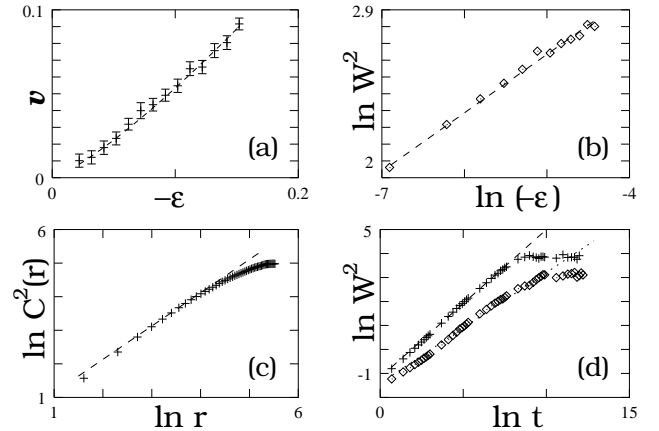


FIG. 3. (a) Plot of the velocity v versus $-\epsilon$ for the symmetric case of the growth model. The dashed line $v = 0.95 * (-\epsilon)^{1.25}$ was obtained by a least-square-fit. (b) DLP of W^2 versus $-\epsilon$ to measure the exponent χ . The dotted line, a guideline to the eye, has slope 0.34. (c) DLP of the height-height correlation function versus distance r at $q = 0.9$. The data are well fit to a straight line with slope $2\zeta = 1$. (d) DLP of W^2 versus t at probabilities $q = 0.5$ and 0.9 (top). The dotted and dashed lines have slopes 0.49 and 0.62(top) to guide to the eye. All plots (a-d) are for the symmetric case of the growth model with $L = 500$, and the data are averaged over 500 configurations.